Journal of Dynamics and Games
©American Institute of Mathematical Sciences
Volume **2**, Number **1**, January **2015**

doi:10.3934/jdg.2015.2.65

pp. **65–87**

DISCRETE TIME DYNAMIC OLIGOPOLIES WITH ADJUSTMENT CONSTRAINTS

Chrystie Burr

Department of Economics
University of Colorado
Boulder, CO 80309-0256, USA

Laura Gardini

Department of Economics, Society, Politics
Università degli Studi di Urbino
61029 Urbino, Italy

Ferenc Szidarovszky

Department of Applied Mathematics
University of Pécs
Pécs, 7624, Hungary

(Communicated by Rabah Amir)

Abstract. A classical n-firm oligopoly is considered first with linear demand and cost functions which has a unique equilibrium. We then assume that the output levels of the firms are bounded in a sense that they are unwilling to make small changes, the output levels are bounded from above, and if the optimal output level is very small then the firms quit producing, which are realistic assumptions in real economies. In the first part of the paper, the best responses of the firms are determined and the existence of infinitely many equilibria is verified. The second part of the paper examines the global dynamics of the duopoly version of the game. In particular we study the stability of the system, the bifurcations which can occur and the basins of attraction of the existing attracting sets, as a function of the speed of adjustment parameter.

1. Introduction.

Assume n firms produce the same product or offer identical service to a homogeneous market. Let x_k denote the output of firm k, $s = \sum_{k=1}^{n} x_k$ the output of the industry. If $p(s)$ is the inverse demand function and $C_k(x_k)$ is the production cost of firm k, then its profit is given as

$$\Pi_k = x_k p(s) - C_k(x_k) \tag{1}$$

In this way a n-person game is defined, where the firms are the players, the set of non-negative real numbers is the strategy set of each player, and the payoff of player k is given by equation (1). This game is one of the most frequently studied models in mathematical economics. A comprehensive summary of the earliest results is given in [16], their multiproduct generalization with case studies are discussed in [17].

2010 *Mathematics Subject Classification.* Primary: 91A06, 91A25, 91A50, 91B55; Secondary: 37G35, 37G15.

Key words and phrases. Dynamic Cournot oligopoly, steady state, bounded output, adjustment constraints, stability, bifurcation.

The studied models were mainly linear making equilibrium and stability analysis relatively simple. The attention recently turned to the analysis of nonlinear models due to the drastically improved computational power. The authors of [3] offer a review of the most recent development in this area.

In this paper, we first consider the baseline Cournot model with no output adjustment constraints (called model I), in which case there is a unique equilibrium. Next, we consider the case (called model II) when it is difficult (costly) for firms to make output adjustments. Thus, we introduce the additional assumption that the firms are not willing to make very small output adjustments, since the small profit increase is insufficient to offset all required fixed adjustment costs in the production process such as difficulties in modifying input contracts or in coordination between divisions within a firm. This "stickiness" in outputs is analogous to the literature on "sticky prices" ([9], [22]) whereas the sticky price is reflected in the speed of adjustment parameter and ours is reflected in the modified best response function. We further assume that the amount of output in each time period is bounded from above due to limited resources, such as physical capacity of the plant, so the output adjustments are also bounded from above. It's also assumed that firms are not willing to produce at a very low output level to avoid fixed operation and maintenance costs. These additional assumptions result in nonlinear, discontinuous best response functions and infinitely many steady states of the dynamic system.

We investigate in particular the dynamics in the duopoly case. We are particularly interested in the attractivity of the fixed point meaning that the trajectory converge to that fixed point. The interesting dynamics occur when the set of fixed points is no longer attracting, at this point, 2-cycles are the only possible attractors; in particular, at least one periodic point (or both) must take on the values introduced in the constrained model II.

The dynamics of model II are particularly interesting from a mathematical point of view as well. Indeed, the model is described by a discontinuous two-dimensional piecewise linear map, with several borders crossing which the system changes its definition, although limited to a rectangular absorbing region of the production phase plane (x_1, x_2). The dynamics associated with piecewise smooth systems is a relatively new research area, and several papers have been dedicated to this subject in the last decade ([27], [7]). This growing interest in nonsmooth dynamics is from both the new theoretical problems with constraints and the applied fields. In fact, many models are described by constrained functions, leading to piecewise smooth systems, continuous or discontinuous. We recall several oligopoly models with different kinds of constraints considered in the books [19] and [3], nonsmooth economic models in [6], [18], [10], [24], financial market modeling in [12], [25], [26], Shelling segregations models in [20], [21], and modeling of multiple-choice in [4], [11], [5].

Model II considered in the present paper is characterized by several constraints, leading to several different partitions of the phase plane in which the system changes definition. Moreover, the definitions in some regions are degenerate, as mapped into points or segments of straight lines. When the existing $2-$cycle has a periodic point colliding with a border of the regions, then a border collision occurs, which in our case is always a *persistent border collision,* as it is simply transformed in a $2-$cycle belonging to different partitions (see [14], [15], [23]).

The structure for the rest of this paper is as follows. Section 2 introduces the model set-ups and Section 3 analyzes the steady state. In Section 4 we investigate the dynamics of the affine duopoly model I, while Section 5 is devoted to the piecewise linear and discontinuous model II. In particular, in subsection 5.1 the symmetric case is fully described, while the proper argumentations are given for the general case in subsection 5.2. Section 6 concludes.

2. Mathematical models.

2.1. The baseline Model I. Assume linear demand, $p(s) = a - bs$ and heterogeneous cost functions, $C_k(x_k) = c_k x_k + d_k,\ k = 1, ..., n$. The profit of firm k is therefore quadratic,

$$\Pi_k = x_k(a - bx_k - bs_k) - (c_k x_k + d_k), \tag{2}$$

which is a strictly concave function in x_k. $s_k = \sum_{\ell \neq k} x_\ell$ denotes the output of the rest of the industry from firm k 's perspective. The profit maximizing quantity x_k^* is derived by simple differentiation,

$$\frac{\partial \Pi}{\partial x_k} = a - 2bx_k - bs_k - c_k = 0,$$

leading to

$$x_k^* = \frac{a - c_k - bs_k}{2b} \ . \tag{3}$$

It is well known that there is a unique equilibrium of this static game.

The dynamic extension of this model with discrete time scales and adjustments toward best responses can be modeled by the discrete system defined as:

$$x_k(t+1) = x_k(t) + K_k \left[\overline{x}_k^*(t+1) - x_k(t)\right] \tag{4}$$

for $k = 1, 2, ..., n$ where $K_k > 0$ for any k is the speed of adjustment parameter of firm k. The usual assumption that $K_k < 1$ models firms with "cautious" behavior, however, more "aggressive" firms may select $K_k > 1$ counting for the continuation of the trend in rival firm's output levels. We also assume that the best response of firm k in the next period, $\overline{x}_k^*(t+1)$ depends only on the aggregated output of the rest of the industry in the current period, $s_k(t)$:

$$\overline{x}_k^*(t+1) = \frac{a - c_k - bs_k(t)}{2b} \ . \tag{5}$$

2.2. Model II with output adjustment constraints (fixed capacity). Assume next that the firms do not want to make adjustment below a certain threshold ϵ_k ("sticky output" constraint) from an initial output level, x_k, and cannot produce outputs greater than a specified (fixed) positive threshold L_k (capacity limit constraint), or smaller than a given small threshold, l_k. That is, if the optimal output falls below this threshold, firm will simply choose not to produce. Based on these additional conditions, the modified best response of firm k becomes

$$\tilde{R}_k\left(s_k, x_k\right) = \begin{cases} x_k & \text{if} \quad |x_k^* - x_k| \leq \epsilon_k \\ L_k & \text{if} \quad x_k^* \geq L_k \\ 0 & \text{if} \quad x_k^* < l_k \\ x_k^* & \quad \text{otherwise} \end{cases} \tag{6}$$

Fig.1 illustrates this function. It can be shown that the two restrictions on a firm's responsiveness to rivals' behavior imply that the firm's reaction curve is

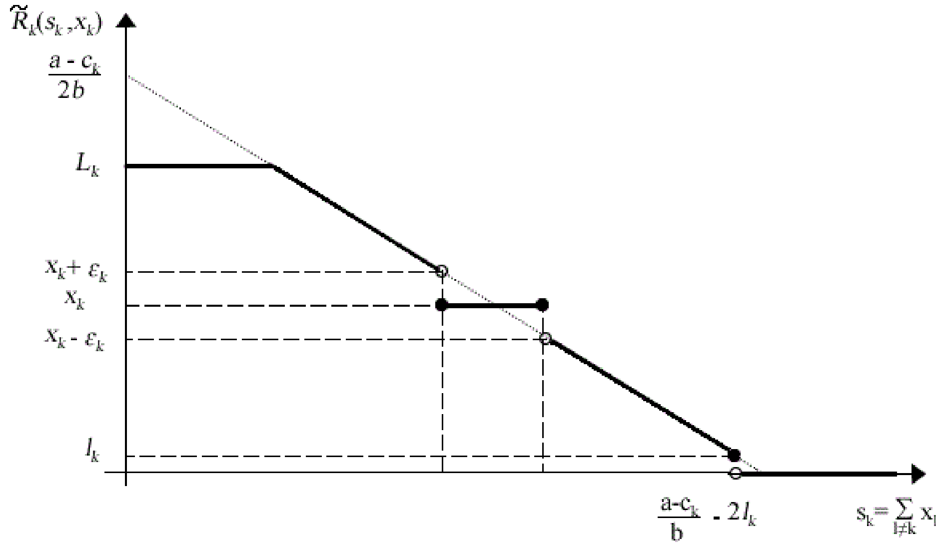

FIGURE 1. Best response function of firm k as given in (6).

still downward sloping although it now has points of discontinuity, always in the form of downward jumps, and is thus no longer globally linear in rivals' output. It follows that the resulting oligopoly game is of strategic substitutes, so that a pure-strategy Nash equilibrium always exists as a consequence of the general properties of submodular games that satisfy a common aggregation property, namely that each firm's profit function depends only on own output and on total rivals' output (see [13] and [1], [2]). We could develop a best response dynamic model based on $\tilde{R}_k$, however, there is no guarantee that the new output levels $x_k(t+1)$ would satisfy the constraints posed in (6). Instead we use a two step process. In the first step, we apply the best response dynamics based on the unconstrained reaction function (3), and then in the second step we enforce condition (6) on the computed output levels.

Therefore, the corresponding dynamic model now has the form,

$$x_k(t+1) = \begin{cases} x_k(t) & \text{if } |\tilde{x}_k(t+1) - x_k(t)| \leq \epsilon_k \\ L_k & \text{if } \tilde{x}_k(t+1) \geq L_k \\ 0 & \text{if } \tilde{x}_k(t+1) < l_k \\ \tilde{x}_k(t+1) & \text{otherweise} \end{cases} \tag{7}$$

where

$$\tilde{x}_k(t+1) = x_k(t) + K_k\left[\overline{x}_k^*(t+1) - x_k(t)\right], \quad k = 1, 2, ..., n. \tag{8}$$

Notice that the function defined in (7) is discontinuous and nonlinear making the equilibrium and stability analysis different with respect to the linear baseline model I.

3. **Steady states.** Consider first the baseline model I defined in (4): an output vector $(\bar{x}_1, \cdots, \bar{x}_n)$, where $\bar{x}_i = x_i(t+1) = x_i(t)$, is a steady state if and only if for all k,

$$\frac{a - c_k - b\sum_{\ell \neq k} \bar{x}_\ell}{2b} = \bar{x}_k$$

implying that

$$\bar{x}_k = \frac{a - c_k - bs}{b}. \tag{9}$$

Summing up equation (9) for all $k = 1, 2, ..., n$, we have

$$\bar{s} = \frac{na - \sum_{\ell=1}^{n} c_\ell - nb\bar{s}}{b}$$

that is,

$$\bar{s} = \frac{na - \sum_{\ell=1}^{n} c_\ell}{(n+1)b} \ . \tag{10}$$

Then from (9) and (10) we can derive the equilibrium output levels of the firms:

$$\bar{x}_k = \frac{a + \sum_{\ell=1}^{n} c_\ell - (n+1)c_k}{(n+1)b}. \tag{11}$$

The attractivity analysis of the linear system in (4) will be given in the next section. Here we only remark that in order to have a fixed point with positive coordinates, we assume that the following condition (h_n) holds:

$$(h_n): \quad a > (n+1)c_k - \sum_{\ell=1}^{n} c_\ell \quad \text{for } k = 1, 2, ..., n \ . \tag{12}$$

Due to the additional constraints, the steady states of model II is different from (11). An output vector $(\bar{x}_1, \cdots, \bar{x}_n)$ is a steady state of the system if and only if for all k,

$$\left| \frac{a - c_k - b\sum_{\ell \neq k} \bar{x}_\ell}{2b} - \bar{x}_k \right| \leq \frac{\epsilon_k}{K_k} \tag{13}$$

which can be rewritten as

$$\frac{a - c_k}{b} - 2\frac{\epsilon_k}{K_k} \leq \sum_{\ell \neq k} \bar{x}_\ell + 2\bar{x}_k \leq \frac{a - c_k}{b} + 2\frac{\epsilon_k}{K_k} \ . \tag{14}$$

Note that the steady state of model I in (11) clearly satisfies these relations which means that the equilibrium quantities in the baseline model will always be one of the solutions in the models with the additional constraints. There are infinitely many steady states in model II since (14) is satisfied by a bounded polyhedron, denoted ER (Equilibria Region, or region of fixed points) as in Figure 2 for the case $n = 2$. In particular, ER belongs to the positive orthant assuming a small enough ϵ_k and by condition (h_n) in (12).

Example 1. Consider a Cournot duopoly, i.e. $n = 2$, then the relations in (14) can be rewritten as

$$\frac{a - c_1}{b} - 2\frac{\epsilon_1}{K_1} \leq x_2 + 2x_1 \leq \frac{a - c_1}{b} + 2\frac{\epsilon_1}{K_1} \tag{15}$$

and

$$\frac{a - c_2}{b} - 2\frac{\epsilon_2}{K_2} \leq x_1 + 2x_2 \leq \frac{a - c_2}{b} + 2\frac{\epsilon_2}{K_2} \ . \tag{16}$$

Fig.2 illustrates the set of feasible solutions of the duopoly example. The equilibrium region ER is determined by the intersections of the straight lines of equations

$$x_2 = -2x_1 + \frac{a - c_1}{b} + \frac{2\epsilon_1}{K_1} \tag{17}$$

$$x_2 = -2x_1 + \frac{a - c_1}{b} - \frac{2\epsilon_1}{K_1} \tag{18}$$

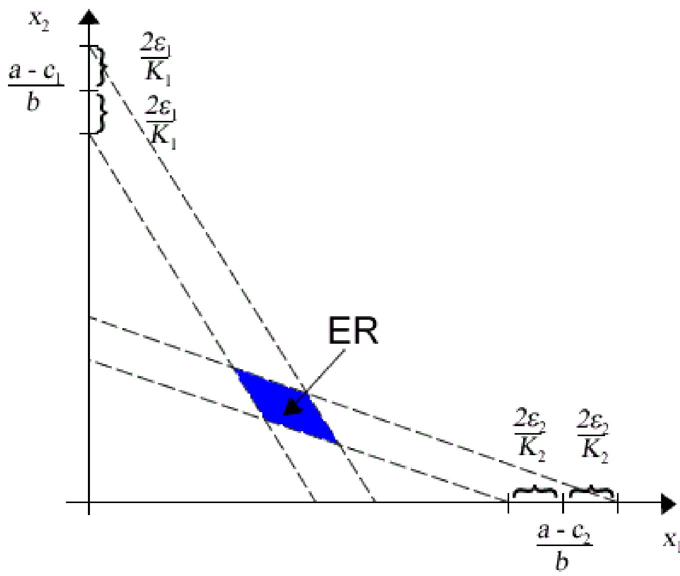

FIGURE 2. Set ER of fixed points for model II.

and

$$x_2 = -\frac{1}{2}x_1 + \frac{a-c_2}{2b} + \frac{\epsilon_2}{K_2} \tag{19}$$

$$x_2 = -\frac{1}{2}x_1 + \frac{a-c_2}{2b} - \frac{\epsilon_2}{K_2} \tag{20}$$

The region ER includes the unique equilibrium, E, of the baseline model. From (11), $E = (x_1^E, x_2^E)$, and

$$\begin{cases} x_1^E = \frac{a+c_2-2c_1}{3b} \\ x_2^E = \frac{a+c_1-2c_2}{3b} \end{cases} \tag{21}$$

Note that E belongs to the positive quadrant $\mathcal{R}_+^2$ as long as condition (h_n) is met, that is,

$$(h_2) \ : \quad a + c_2 - 2c_1 > 0 \text{ and } a + c_1 - 2c_2 > 0 \ . \tag{22}$$

In the next two sections, we consider in detail the dynamic behavior of the duopoly models I and II, respectively, assuming that condition (h_2) in (22) holds. We show that the system with the bounded output adjustments, due to the constraints of the model, is in some sense more stable than the baseline model. The intuition behind this observation is that despite the stability condition of E and of ER is the same in both models, model II has bounded dynamics even when ER is not attracting.

4. **Stability analysis and dynamics of Model I.** Let us explicitly rewrite the best response dynamics for $n = 2$: a point (x_1, x_2) is mapped into (x_1', x_2') by

$$\begin{cases} x_1' = f_1(x_1, x_2) = (1 - K_1)x_1 - \frac{K_1}{2}x_2 + \frac{a-c_1}{2b}K_1 \\ x_2' = f_2(x_1, x_2) = (1 - K_2)x_2 - \frac{K_2}{2}x_1 + \frac{a-c_2}{2b}K_2 \end{cases} \tag{23}$$

which is a linear, or more precisely, an *affine* model. We can refer to it as a linear model, following the common usage in dynamical systems, as it is topologically conjugate with a linear model after a change of variable setting the fixed point of (23) into the origin. Its fixed point, $E = (x_1^E, x_2^E)$, has been given explicitly in (21). Notice that its position in the phase plane (x_1, x_2) does not depend on K_1 and K_2 while the stability of the equilibrium E clearly depends on K_1 and K_2. From the Jacobian determinant of the linear map in (23), we find that the characteristic polynomial is given by

$$P(\lambda) = \lambda^2 - tr\lambda + D \tag{24}$$

where

$$\begin{aligned} tr &= 2 - (K_1 + K_2) \\ D &= 1 - (K_1 + K_2) + \frac{3}{4}K_1K_2. \end{aligned} \tag{25}$$

The sufficient stability conditions of E are:

$$\begin{aligned} P(1) &= 1 - tr + D = \frac{3}{4}K_1K_2 > 0 \\ P(-1) &= 1 + tr + D = 4 - 2(K_1 + K_2) + \frac{3}{4}K_1K_2 > 0 \\ D &< 1 : \frac{3}{4}K_1K_2 < (K_1 + K_2) \end{aligned} \tag{26}$$

While $P(1) > 0$ is always satisfied, condition $P(-1) > 0$ is satisfied iff

1. $K_1 < \frac{8}{3}$ and $K_2 < \frac{16-8K_1}{8-3K_1}$
2. $K_1 > \frac{8}{3}$ and $K_2 > \frac{16-8K_1}{8-3K_1}$.

Meanwhile, condition $D < 1$ is satisfied iff

1. $K_1 < \frac{4}{3}$ and $K_2 > 0$
2. $K_1 > \frac{4}{3}$ and $K_2 < \frac{4K_1}{3K_1-4}$.

These conditions can be summarized in Fig.3. We denote by S the stability region of the fixed point E, which is bounded by an arc of hyperbola (denoted F in Fig.3). At the bifurcation curve F of equation $K_2 = \frac{16-8K_1}{8-3K_1}$ one eigenvalue is equal to -1.

For values of (K_1, K_2) outside of the stability region S, the fixed point is either a saddle or a repelling node. Recall that in a linear model when the equilibrium is a repelling node then all the trajectories, apart from the fixed point, are divergent; when the equilibrium is a saddle, all the trajectories are divergent except for the fixed point and its stable set, which is the eigenvector associated with the stable eigenvalue. We now determine the eigenvalues and eigenvectors of the linear system, model I, which will also be useful for the dynamic analysis of model II. In general, given a 2x2 Jacobian matrix

$$J = \begin{bmatrix} J_{11} & J_{12} \\ J_{21} & J_{22} \end{bmatrix}$$

with $J_{12} \neq 0$, $J_{21} \neq 0$ and real eigenvalues, we can find the eigenvalues, $\lambda_\pm$, and the eigenvectors, $e_\pm$, with slopes $m_\pm$ by solving the system,

$$\begin{bmatrix} J_{11} & J_{12} \\ J_{21} & J_{22} \end{bmatrix} \begin{bmatrix} 1 \\ m_\pm \end{bmatrix} = \lambda_\pm \begin{bmatrix} 1 \\ m_\pm \end{bmatrix},$$

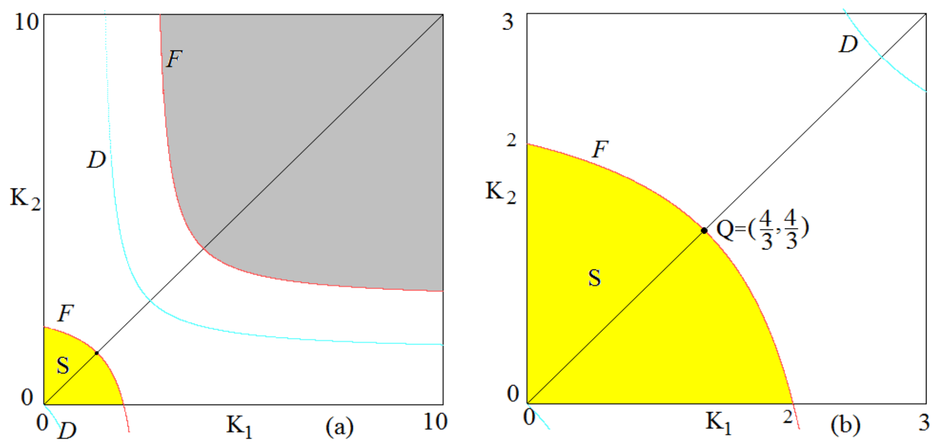

FIGURE 3. Stability region of model I in the parameter plane (K_1, K_2) in yellow. In (b) the enlargement of (a) is shown.

or, equivalently,

$$\left\{ \begin{array}{c} J_{11} + m_{\pm} J_{12} = \lambda_{\pm} \\ J_{21} + m_{\pm} J_{22} = \lambda_{\pm} m_{\pm} \end{array} \right. ,$$

so to find

$$m_{\pm} = \frac{J_{22} - J_{11} \pm \sqrt{(J_{22} - J_{11})^2 + 4 J_{12} J_{21}}}{2 J_{12}} \tag{27}$$
$$\lambda_{\pm} = J_{11} + m_{\pm} J_{12}.$$

For the specific duopoly model, by substituting $J_{11} = 1 - K_1$, $J_{12} = -\frac{K_1}{2}$, $J_{21} = -\frac{K_2}{2}$ and $J_{22} = 1 - K_2$, we obtain:

$$m_{\pm} = \frac{K_2 - K_1 \mp \sqrt{(K_2 - K_1)^2 + K_2 K_1}}{K_1} \tag{28}$$
$$\lambda_{\pm} = 1 - \frac{K_2 + K_1}{2} \pm \frac{\sqrt{(K_2 - K_1)^2 + K_2 K_1}}{2}.$$

It can be seen that

$$m_{+} = \frac{(K_2 - K_1) - \sqrt{(K_2 - K_1)^2 + K_2 K_1}}{K_1} < 0,$$

while

$$m_{-} = \frac{(K_2 - K_1) + \sqrt{(K_2 - K_1)^2 + K_2 K_1}}{K_1} > 0.$$

The eigenvalue $\lambda_{-} = 1 - \frac{K_2 + K_1}{2} - \frac{\sqrt{(K_2 - K_1)^2 + K_2 K_1}}{2}$ becomes unstable when crossing the value $\lambda_{-} = -1$ and the bifurcation occurs for $K_2 = \frac{16 - 8K_1}{8 - 3K_1}$. If $K_1 > 2$, the system is unstable regardless of the value of K_2.

If $K_1 < 2$, the system is stable only if K_2 is small enough, i.e. when the point (K_1, K_2) belongs to region S (the yellow region in Fig.3). If K_2 is large enough, i.e. (K_1, K_2) is outside region S, then the fixed point E is a saddle since the eigenvalue $\lambda_{+} = 1 - \frac{K_2 + K_1}{2} + \frac{\sqrt{(K_2 - K_1)^2 + K_2 K_1}}{2}$ never bifurcates.

For $K_1 > 2$, λ_+ also becomes negative and unstable when crossing the value $\lambda_+ = -1$ for $K_2 = \frac{16-8K_1}{8-3K_1}$. This occurs on the right side of the vertical asymptote, that is, on the right branch of the hyperbola in Fig.3a. For (K_1, K_2) in the gray region in Fig.3a, both eigenvalues are negative with $\lambda_\pm < -1$, and E is therefore a repelling node.

In the special case of equal speed of adjustments $K = K_1 = K_2$, the eigenvectors $e_\pm$ have constant slopes $m_\pm$, as in fact we have:

$$m_+ = -1 \text{ (associated with the eigenvalue } \lambda_+ = 1 - \frac{K}{2})$$
$$m_- = +1 \text{ (associated with the eigenvalue } \lambda_- = 1 - \frac{3K}{2})$$

The fixed point E is globally attracting if $K < \frac{4}{3}$. At $K = \frac{4}{3}$ (see the point Q in the enlargement of Fig.3b), one eigenvalue (λ_-) becomes -1. For $K > \frac{4}{3}$ the eigenvalues are $\lambda_\pm < -1$, and E is a repelling node.

5. **Stability analysis and dynamics of Model II.** In the duopolistic competition, a point (x_1, x_2) is mapped by model II into $(x_1', x_2') = T(x_1, x_2)$ where

$$x_1' = \begin{cases} x_1 & \text{if} \quad |\widetilde{x}_1 - x_1| \le \epsilon_1 \\ L_1 & \text{if} \quad \widetilde{x}_1 \ge L_1 \\ 0 & \text{if} \quad \widetilde{x}_1 < l_1 \\ \widetilde{x}_1 & \quad \text{otherwise} \end{cases} \tag{29}$$

$$x_2' = \begin{cases} x_2 & \text{if} \quad |\widetilde{x}_2 - x_2| \le \epsilon_2 \\ L_2 & \text{if} \quad \widetilde{x}_2 \ge L_2 \\ 0 & \text{if} \quad \widetilde{x}_2 < l_2 \\ \widetilde{x}_2 & \quad \text{otherwise} \end{cases} \tag{30}$$

and

$$\begin{cases} \widetilde{x}_1 = f_1(x_1, x_2) = (1 - K_1)x_1 - \frac{K_1}{2}x_2 + \frac{a-c_1}{2b}K_1 \\ \widetilde{x}_2 = f_2(x_1, x_2) = (1 - K_2)x_2 - \frac{K_2}{2}x_1 + \frac{a-c_2}{2b}K_2 \end{cases} \tag{31}$$

We can rewrite the piecewise linear map more explicitly as follows:

$$x_1' = \begin{cases} x_1 & \text{if} \quad \left|\frac{a-c_1-bx_2}{2b} - x_1\right| \le \frac{\epsilon_1}{K_1} \\ L_1 & \text{if} \quad \widetilde{x}_1 \ge L_1 \\ 0 & \text{if} \quad \widetilde{x}_1 < l_1 \\ \widetilde{x}_1 & \text{if} \quad l_1 \le \widetilde{x}_1 < L_1 \text{ and } |\widetilde{x}_1 - x_1| > \epsilon_1 \end{cases} \tag{32}$$

$$x_2' = \begin{cases} x_2 & \text{if} \quad \left|\frac{a-c_2-bx_1}{2b} - x_2\right| \le \frac{\epsilon_2}{K_2} \\ L_2 & \text{if} \quad \widetilde{x}_2 \ge L_2 \\ 0 & \text{if} \quad \widetilde{x}_2 < l_2 \\ \widetilde{x}_2 & \text{if} \quad l_2 \le \widetilde{x}_2 < L_2 \text{ and } |\widetilde{x}_2 - x_2| > \epsilon_2 \end{cases} \tag{33}$$

As shown in the previous section there is no unique fixed point but instead a whole region ER of fixed points, which includes the equilibrium E of the baseline model. By its definition, the map takes on different values depending on the position of a point (x_1, x_2) in the phase plane. We can thus subdivide the phase plane into regions R_j $j = 1, 2, \ldots$, in each of which the map takes different definitions. These regions R_j are bounded by segments of the straight lines satisfying the following equations:

$$\begin{aligned}(r_a) &: \widetilde{x}_1 = L_1 \\ (r_b) &: \widetilde{x}_1 = l_1 \\ (r_c) &: \widetilde{x}_2 = L_2 \\ (r_d) &: \widetilde{x}_2 = l_2\end{aligned} \tag{34}$$

that is, in explicit form:

$$\begin{aligned}(r_a) &: (1-K_1)x_1 - \frac{K_1}{2}x_2 + K_1(\frac{a-c_1}{2b}) = L_1 \\ (r_b) &: (1-K_1)x_1 - \frac{K_1}{2}x_2 + K_1(\frac{a-c_1}{2b}) = l_1 \\ (r_c) &: (1-K_2)x_2 - \frac{K_2}{2}x_1 + K_2(\frac{a-c_2}{2b}) = L_2 \\ (r_d) &: (1-K_2)x_2 - \frac{K_2}{2}x_1 + K_2(\frac{a-c_2}{2b}) = l_2\end{aligned} \tag{35}$$

Let us denote R_1 the region bounded by segments of all the four lines, in which the map is defined as in the linear model I except for the region ER of fixed points. Consider the regions of interests which are defined as[1]

$$\begin{array}{lcl} R_1 &=& \{(x_1,x_2)\,|l_1 < \widetilde{x}_1 \le L_1 \text{ and } l_2 < \widetilde{x}_2 \le L_2\} \\ R_2 &=& \{(x_1,x_2)\,|l_1 < \widetilde{x}_1 \le L_1 \text{ and } \widetilde{x}_2 < l_2\} \\ R_3 &=& \{(x_1,x_2)\,|\widetilde{x}_1 < l_1 \text{ and } l_2 < \widetilde{x}_2 \le L_2\} \\ R_4 &=& \{(x_1,x_2)\,|\widetilde{x}_1 < l_1 \text{ and } \widetilde{x}_2 < l_2\} \\ R_5 &=& \{(x_1,x_2)\,|l_1 < \widetilde{x}_1 \le L_1 \text{ and } \widetilde{x}_2 > L_2\} \\ R_6 &=& \{(x_1,x_2)\,|\widetilde{x}_1 > L_1 \text{ and } \widetilde{x}_2 > L_2\} \\ R_7 &=& \{(x_1,x_2)\,|\widetilde{x}_1 > L_1 \text{ and } l_2 < \widetilde{x}_2 \le L_2\}\,. \end{array} \tag{36}$$

The map in each region is defined as

$$\begin{array}{ll} (x_1,x_2) \in R_1 \backslash ER & : (x_1', x_2') = (\widetilde{x}_1, \widetilde{x}_2) = (f_1(x_1,x_2), f_2(x_1,x_2)) \\ (x_1,x_2) \in R_2 & : (x_1', x_2') = (\widetilde{x}_1, 0) = (f_1(x_1,x_2), 0) \\ (x_1,x_2) \in R_3 & : (x_1', x_2') = (0, \widetilde{x}_2) = (0, f_2(x_1,x_2)) \\ (x_1,x_2) \in R_4 & : (x_1', x_2') = (0,0) \\ (x_1,x_2) \in R_5 & : (x_1', x_2') = (\widetilde{x}_1, L_2) = (f_1(x_1,x_2), L_2) \\ (x_1,x_2) \in R_6 & : (x_1', x_2') = (L_1, L_2) \\ (x_1,x_2) \in R_7 & : (x_1', x_2') = (L_1, \widetilde{x}_2) = (L_1, f_2(x_1,x_2)). \end{array} \tag{37}$$

From the definition of the map, the rectangle

$$\mathcal{D} = [0, L_1] \times [0, L_2] \tag{38}$$

is absorbing, as it follows immediately from (32) and (33) that any point of the plane is mapped in $\mathcal{D}$ in one iteration and an orbit cannot escape from it. $\mathcal{D}$ is therefore the region of interest.

In general, depending on the values of the parameters, only a few of the regions R_j for $j = 1, 2, ...$ may have a portion, or subregion, present in $\mathcal{D}$, or $R_j \cap \mathcal{D} \neq \varnothing$, as

[1] There are other possible regions. However, we focus on these seven regions since we are only interested in the positive quadrant of the phase plane, $\mathcal{R}_+^2$.

shown in Fig.4. In Fig.4a only two regions have points in $\mathcal{D}$, while in Fig.4b there are four regions.

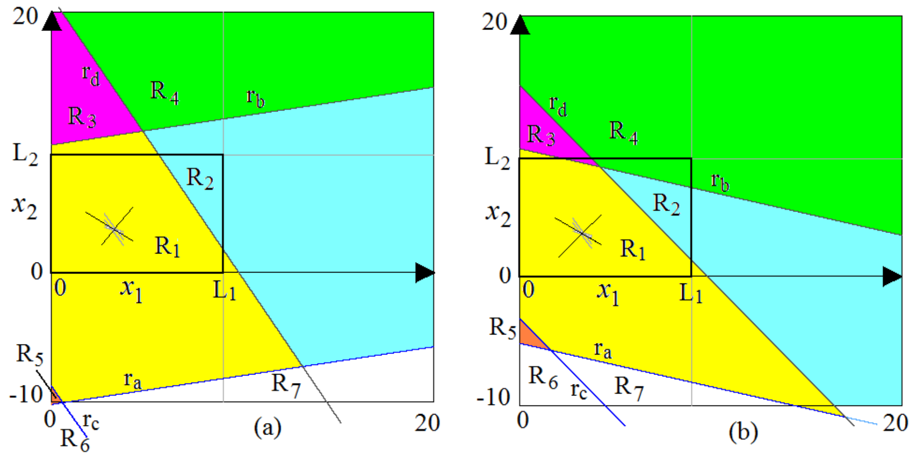

FIGURE 4. Regions of the phase plane, at the parameter values $L_1 = L_2 = 9$, $l_1 = l_2 = .01$, $\epsilon_1 = \epsilon_2 = 0.1$, $c_1 = c_2 = 0.2$, $a = 10$, $b = 1$, and $K_1 = 0.9$, $K_2 = 1.3$ in (a), $K_1 = 1.2$, $K_2 = 1.5$ in (b). Inside region R_1 segments of the 4 lines determining region of fixed points ER are also shown, together with the eigenvectors of the fixed point E inside ER.

Since we assume ϵ_1 and ϵ_2 are small enough, ER is internal to the positive quadrant and in the R_1 region. Therefore, the fixed points are surrounded by a region where the mapping is the same as in the baseline model. Fig.4 also shows the segments which are intersecting to give the region ER of fixed points (and $E \in ER$), and segments of the eigenvectors e_+ and e_- of E, which are also invariant lines for the linear map defined in $R_1 \backslash ER$.

A fixed point p is *stable* if there exist a neighborhood $U_1(p)$ and a neighborhood $U_2(p)$, $U_1(p) \subset U_2(p)$ such that any initial condition (i.c. for short henceforth) in $U_1(p)$ has the trajectory inside $U_2(p)$. Meanwhile, p is *attracting* if it is stable and the trajectory with any i.c. in $U_1(p)$ converges to p. It is clear that each fixed point belonging to ER can be stable but not attracting. Since ER is surrounded by points with the same mapping as in model I, we have that as long as the K_1 and K_2 belong to the stability region S, determined for model I, the neighborhoods $U_1(p)$ and $U_2(p)$ exist for any $p \in ER$ and any i.c. in $U_1(p)$ has the trajectory converging to a point in ER. Thus ER consists of points which are stable but not attracting, while the invariant set ER itself is an "invariant attracting set". We therefore have shown that the stability region of model II in the parameter space (K_1, K_2) is the same as for model I, and we can state the following

Proposition 1 (*local stability*)**.** *Let* $(K_1, K_2) \in S$ *(stability region of model I), then the invariant set* ER *of model II is attracting.*

In addition, similar to the fixed point E being globally stable when (K_1, K_2) is in S, ER is globally attracting for the same (K_1, K_2) range. As remarked above, any point of the plane is mapped in one iteration in the rectangle $\mathcal{D}$ in (38). Clearly when E is stable then all the points in R_1 with a trajectory in R_1 will end in ER. When any of the regions R_j satisfying $R_j \cap \mathcal{D} \neq \varnothing$ exists, its points are mapped on the borders of $\mathcal{D}$ and the mappings on these border points are the same as in model I and therefore are contractions. For example, considering Fig.4a when ER is attracting and $R_2 \cap \mathcal{D} \neq \varnothing$. Then all the points of $R_2 \cap \mathcal{D}$ are mapped into the x_1−axis, on the border of $\mathcal{D}$, obtaining a point $(x_1', x_2') = (f_1(x_1, x_2), 0)$ which can either be in R_1 or in R_2 again. The contraction f_1 is applied until the point enters R_1; thus ER is globally attracting. We will not provide a rigorous proof of the global attractivity of ER when $(K_1, K_2) \in S$ because of the many possible cases to comment, but in all scenarios the reasoning is the same.

When the parameters K_1 and K_2 are outside of the stability region and E is a saddle, the points around ER behave as in the linear map thus the stable set of ER can be defined, and ER can declassified as an "unstable" invariant set having the same properties of a saddle. This means that there are points (a set of positive Lebesgue measure) in the phase plane whose trajectories ultimately end in ER, which constitute the stable set of ER. Meanwhile there are also points in a neighborhood of ER that diverge away from the neighborhood. Clearly when E is a repelling node then locally all the points around ER diverge, and ER can be defined as a locally repelling invariant set. Similarly we can explain the dynamic behavior at the bifurcation value, when the parameters K_1 and K_2 are on the boundary F of the stability region, and one eigenvalue is $\lambda_- = -1$. The related eigenvector e_- leads the points in R_1 to a segment of cycles of period 2 (while the other eigenvector e_+ is inside the stable set of ER).

Fig.4b shows an example where E is a saddle. In this case, the eigenvector e_- associated with the eigenvalue $\lambda_- < -1$ plays an important role at the bifurcation value (when $\lambda_- = -1$). That is, when $\lambda_- = -1$, the points of the eigenvector e_- belonging to $R_1 \backslash ER$ include two segments filled with 2-cycles (stable but not attracting). In general the 2-cycle at the external side of these segments has one point on some border, which can be either a border of the region $\mathcal{D}$ or a border line r_k ($k \in \{a, b, c, d\}$). *This determines which regions will contain the attracting 2-cycle which exists after the bifurcation* (when $\lambda_- < -1$).

It is worth noting that the map is defined either by constant values or by linear functions (as explicitly reported in (37)). Therefore, when the invariant set ER is unstable, the map cannot have an attracting set in one single region, that is, the possible attractors are obtained only by the piecewise definition of the map, and must necessarily have points in two different regions. In our specific model II, the system can only have 2-cycles as invariant stable sets. In addition, due to the particular structure of the functions in (37), at least one periodic point of the attracting 2-cycle must belong to the border of $\mathcal{D}$ (i.e. must include one of the constants $x_2 = 0$, $x_2 = L_2$, $x_1 = 0$, $x_1 = L_1$), or both belong to the border of $\mathcal{D}$.

As stated above, for $\lambda_- < -1$ and $\lambda_+ > -1$ (i.e. when E is a saddle)), besides an attracting 2-cycle, there exists a set of points (of positive Lebesgue measure) which are mapped into ER in a finite number of iterations, which is called stable set of ER, $W^s(ER)$. Clearly, this stable set includes segments of the eigenvector e_+ of E, at least the portions in region R_1, as well as all the other points in a neighborhood of e_+ belonging to the invariant curves of model I crossing ER, that is, points which are mapped (also in model II) into ER, where they will be fixed.

To comment on the existence of some border collision bifurcations which characterize the 2-cycles when ER is unstable, we start with the symmetric case and establish a few properties before analyzing the general case.

5.1. **Model II in the symmetric case.**

Property 1 (*first symmetry*). *Let $L \equiv L_1 = L_2$, $l \equiv l_1 = l_2$, $c \equiv c_1 = c_2$ and $\epsilon \equiv \epsilon_1 = \epsilon_2$. Let the speed of adjustment parameters have the values $(K_1, K_2) = (\xi, \eta)$ and let $\{(a(t), b(t)),\ t > 0\}$ be the trajectory associated with the initial condition $(a(0), b(0))$. Then $\{(b(t), a(t)),\ t > 0\}$ is the trajectory associated with the initial condition $(b(0), a(0))$ when the parameters have the values $(K_1, K_2) = (\eta, \xi)$.*

That is, via the change of variable $x_2 := x_1$ and $x_1 := x_2$ we have the same dynamics when K_1 and K_2 are interchanged.

As a particular case of Property 1 we have another property when $K_1 = K_2$ (on the diagonal of the two-dimensional parameter plane in Fig.3):

Property 2 (*second symmetry*). *Let $L \equiv L_1 = L_2$, $l \equiv l_1 = l_2$, $c \equiv c_1 = c_2$, $\epsilon \equiv \epsilon_1 = \epsilon_2$ and $K \equiv K_1 = K_2$. Then, besides the symmetry of the trajectories as stated in Property 1, we have that map T is invariant on the diagonal, d, of the phase plane, and its restriction to d is a one-dimensional system $x(t+1) = T_d(x(t))$ $(x = x_1 = x_2)$ given in (39) and (40).*

In fact, from the initial conditions $x(0) = x_1(0) = x_2(0)$, we have $x(t) = x_1(t) = x_2(t)$ for any integer $t > 0$. The iterates are given by the one-dimensional map $x(t+1) = T_d(x(t))$ defined as follows:

$$T_d(x) = \begin{cases} x & \text{if} \quad |\widetilde{x} - x| \leq \epsilon \\ L & \text{if} \quad \widetilde{x} \geq L \\ 0 & \text{if} \quad \widetilde{x} \leq l \\ \widetilde{x} & \quad \text{otherwise} \end{cases} \tag{39}$$

where

$$\widetilde{x} = f_1(x, x) = f_2(x, x) = (1 - \frac{3}{2}K)x + K\frac{a-c}{2b} \tag{40}$$

5.1.1. *Dynamics along the diagonal d.* We can immediately see that as long as $0 < K \leq \frac{2}{3}$ the straight line represented by $\widetilde{x} = f_i(x, x)$ in (40) has a non-negative slope and smaller than 1. Therefore, the mapping T_d has a segment of fixed points in

$$ER_d = [x^E - \frac{2\epsilon}{3K}, x^E + \frac{2\epsilon}{3K}], \tag{41}$$

where $x^E = \frac{a-c}{3b}$ is the same value occurring for the fixed point in model I, and the segment ER_d is globally attracting. For $K > \frac{2}{3}$ the straight line $\widetilde{x} = f_i(x, x)$ has a negative slope, and the qualitative graph of the one-dimensional map T_d is shown in Fig.5. The map T_d still has the segment of fixed points $ER_d = [x^E - \frac{2\epsilon}{3K}, x^E + \frac{2\epsilon}{3K}]$. For $x > p_l$, where

$$p_l = \frac{2l}{2-3K} - \frac{K(a-c)}{b(2-3K)} = \frac{2}{3K-2}(K\frac{a-c}{2b} - l), \tag{42}$$

the map is constant and equal to 0. Based on the position of the vertical intercept, we can further analyze two cases. One is associated with $K(\frac{a-c}{2b}) < L$; here the production limit is not binding as shown in Fig.5a, while the second case refers to

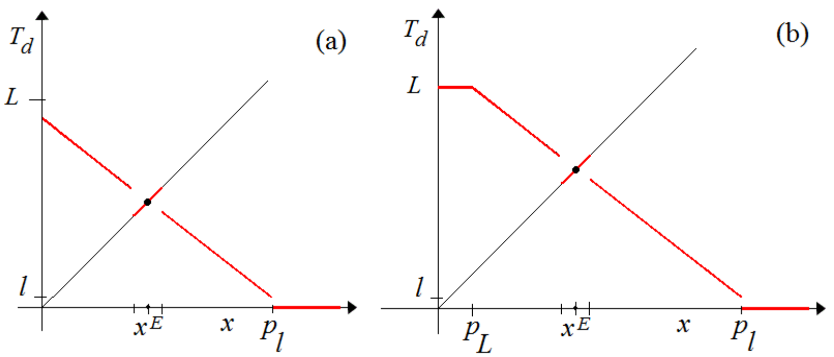

FIGURE 5. Qualitative graph of the one dimensional map T_d. In (a) when $f_i(0,0) = K(\frac{a-c}{2b}) < L$, in (b) when $f_i(0,0) = K(\frac{a-c}{2b}) > L$.

$K(\frac{a-c}{2b}) > L$, so that the upper capacity limit constraint is binding as shown in Fig.5b. Therefore, the mapping is constant and equal to L for $0 < x \leq p_L$, where

$$p_L = \frac{2L}{2-3K} - \frac{K(a-c)}{b(2-3K)} = \frac{2}{3K-2}(K\frac{a-c}{2b} - L). \tag{43}$$

The dynamic behavior of the one-dimensional map T_d is straightforward to analyze.

Case (i) (Attractivity). For $0 < K < \frac{4}{3}$, the segment ER_d of fixed points is globally attracting - and independently of the shape of the map, that is, both for $0 < K \leq \frac{2}{3}$ and for $\frac{2}{3} < K < \frac{4}{3}$.

At the bifurcation value $K = \frac{4}{3}$ we can have different dynamic behaviors, leading to two different attracting 2-cycles after the bifurcation, which can be completely described as follows.

Case (ii) $(K\frac{a-c}{2b} < L$ at $K = \frac{4}{3})$. At $K = \frac{4}{3}$ we have $T_d(0) = 2(\frac{a-c}{3b}) = 2x^E < L$, and $p_l = 2(\frac{a-c}{3b}) - l < T_d(0)$. In this case the segment $(x^E + \frac{\epsilon}{2}, p_l]$ is filled with periodic points of period 2, and it is mapped in the segment $[l, x^E - \frac{\epsilon}{2})$. Moreover, from $p_l < T_d(0)$ we have that at the bifurcation value the points $0 - T_d(0)$, that is $0 - 2(\frac{a-c}{3b})$, belong to a $2-$cycle, and it is the only one surviving after the bifurcation. In fact, for $K > \frac{4}{3}$ the map has a global attractor, the unique $2-$cycle with periodic points 0 and $T_d(0) = f_i(0,0) = K(\frac{a-c}{2b})$. This holds as K increases as long as a border collision bifurcation occurs (at $K\frac{a-c}{2b} = L$). When $K > \frac{2bL}{a-c}$, the globally attracting 2-cycle is then given by the two extrema: $0 - L$.

Case (iii) $(K\frac{a-c}{2b} > L$ at $K = \frac{4}{3})$. At $K = \frac{4}{3}$ we have $T_d(0) = L < K\frac{a-c}{2b}$. In this case the segment $(x^E + \frac{\epsilon}{2}, L]$ is filled with periodic points of period 2, and it is mapped in the segment $[2x^E - L, x^E - \frac{\epsilon}{2})$. In particular, the $2-$cycle on the border having periodic points L and $T_d(L) = 2x^E - L$, is the only one which will survive after the bifurcation. For $K > \frac{4}{3}$ the map has a global attractor, the unique $2-$cycle with periodic points L and $T_d(L) = f_i(L,L) = \frac{2-3K}{2}L + K\frac{a-c}{2b}$. This holds as K increases until $L = p_l$. Therefore, for $K > \frac{2b(L-l)}{3bL-a+c}$, the globally attracting $2-$cycle is given by the two extrema: $0 - L$.

The transition case between (ii) and (iii) occurs when $K\frac{a-c}{2b} = L$ at $K = \frac{4}{3}$, then at the bifurcation value $K = \frac{4}{3}$ all the points not fixed belong to 2−cycles, that is $(x^E + \frac{\epsilon}{2}, L]$ is mapped into $[0, x^E - \frac{\epsilon}{2})$, and for any $K > \frac{4}{3}$ the attracting 2−cycle is given by the two corner points $(0,0) - (L, L)$.

5.1.2. *Dynamics outside the diagonal d.* When the initial conditions for the two firms are not the same, we need to consider the two-dimensional map T. The region ER of fixed points includes the segment ER_d of T_d on the diagonal of the phase plane (x_1, x_2), inside which there is also $E = (x^E, x^E)$. Recall that in this symmetric case of equal speed of adjustments $K = K_1 = K_2$ the eigenvectors $e_\pm$ have constant slopes $m_+ = -1$ (associated with the eigenvalue $\lambda_+ = 1 - \frac{K}{2}$) and $m_- = +1$ (associated with the eigenvalue $\lambda_- = 1 - \frac{3K}{2}$), corresponding to the main diagonal d in the phase plane, which is invariant and on which the restriction is the one-dimensional map T_d described above. The intersection point P_l between the straight lines (r_b) and (r_d) is given by

$$P_l = (p_l, p_l) \tag{44}$$

where p_l has been defined for the one-dimensional map T_d in (42), while the intersection point P_L between the straight lines (r_a) and (r_c) is given by

$$P_L = (p_L, p_L) \tag{45}$$

where p_L has been defined for the one-dimensional map T_d in (43).

Case (i) (Attractivity). For $0 < K < \frac{4}{3}$, the region ER of fixed points is globally attracting, independently of the shape of the map T_d on the diagonal, that is, for both $0 < K \leq \frac{2}{3}$ and $\frac{2}{3} < K < \frac{4}{3}$. In fact, when $K < \frac{2}{3}$ the points P_l and P_L are external to the rectangle $\mathcal{D}$ so that $\mathcal{D}$ belongs to R_1; for other ranges of K, the points P_l or P_L may be internal to the rectangle $\mathcal{D}$. However, the points of $\mathcal{D}$ either belongs to R_1 or are mapped into R_1 in one iteration. For example, Fig.6a and Fig.8a show two examples in the different Cases (ii) and (iii). We can see that in both examples, the regions $R_j \cap \mathcal{D} \neq \varnothing$ with $R_j \neq R_1$, are mapped on borders of $\mathcal{D}$ belonging to R_1 leading to the global attractivity of ER.

At the bifurcation value, $K = \frac{4}{3}$ $(\lambda_- = -1)$, the existing 2−cycles belong to the main diagonal and thus are related to those determined for the map T_d. For $K > \frac{4}{3}$ and $\lambda_+ > -1$ the main diagonal is attracting, apart from ER_d, and the existing attractor is the 2−cycle on the main diagonal determined for the one-dimensional map T_d.

Case (ii) ($K\frac{a-c}{2b} < L$ at $K = \frac{4}{3}$). The intersection point between the straight lines (r_b) and (r_d) is on the diagonal, given by $P_l = (p_l, p_l)$ where p_l has been defined in (42) and

$$(f_i(0,0), f_i(0,0)) = (K\frac{a-c}{2b}, K\frac{a-c}{2b}). \tag{46}$$

At the bifurcation value $K = \frac{4}{3}$ we have $(f(0,0), f(0,0)) = (2\frac{a-c}{3b}, 2\frac{a-c}{3b}) = 2E$, and $P = (p_l, p_l) = (2\frac{a-c}{3b} - l, 2\frac{a-c}{3b} - l)$ which is smaller than $(f_i(0,0), f_i(0,0))$ on the diagonal (as $(2\frac{a-c}{3b} - l) < 2\frac{a-c}{3b}$). Therefore the segment bounded by the points $(x^E + \frac{\epsilon}{2}, x^E + \frac{\epsilon}{2})$ and $P = (p_l, p_l)$ is filled with periodic points of period 2, and it is mapped in the segment bounded by (l, l) and $(x^E - \frac{\epsilon}{2}, x^E - \frac{\epsilon}{2})$, and $(f_i(0,0), f_i(0,0))$ belongs to region R_4 so that

$$(0,0) - (2\frac{a-c}{3b}, 2\frac{a-c}{3b})$$

is a 2−cycle of the map belonging to the regions $R_1 - R_4$, surviving after the bifurcation. That is, the attracting 2−cycle of the map *after the bifurcation* is $(0,0) - (f_i(0,0), f_i(0,0))$:

$$(0,0) - (K\frac{a-c}{2b}, K\frac{a-c}{2b}) \tag{47}$$

Fig.6b shows an example of this. As discussed above, other than this attracting cycle on the diagonal, a stable set $W^s(ER)$ consisting of points of the plane whose trajectory ends in ER in a finite number of steps also exists (and thus $W^s(ER)$ includes the portion of e_+ in region R_1).

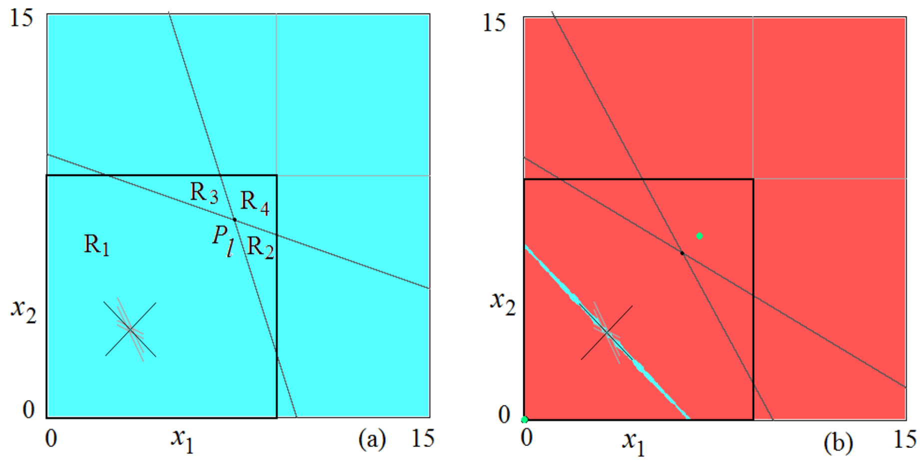

FIGURE 6. Regions of the phase plane in case (ii), at the parameter values $L = 9$, $l = .01$, $\epsilon = 0.1$, $c = 0.2$, $a = 10$, $b = 1$, and $K = 0.9$ in (a), $K = 1.4$ in (b). Inside region R_1 segments of the 4 lines determining ER are also shown, together with the eigenvectors of E. In (a) ER is globally attracting. In (b) the stable set $W^s(ER)$ is shown in azure while the basin of attraction of the 2-cycle $(0,0)-(K\frac{a-c}{2b}, K\frac{a-c}{2b})$ is given in red.

A border collision takes place when $(0,0)$ merges with P_L (i.e. when $p_L = 0$) or, equivalently, when the other periodic point reaches the extremum of $\mathcal{D}$, $(K\frac{a-c}{2b}, K\frac{a-c}{2b}) = (L,L)$. This occurs when $K = \frac{2bL}{a-c}$, after which the 2−cycle is given by the corner points $(0,0) - (L,L)$, see an example in Fig.7a. The stable set $W^s(ER)$ is larger than ER as long as E is a saddle. At $K = 4$ the second eigenvalue bifurcates, $\lambda_+ = -1$, so that for $K > 4$ the invariant set ER becomes repelling, and all the other points converge to the 2−cycle $(0,0) - (L,L)$, see an example in Fig.7b. The attracting 2−cycle always attracts all the points not belonging to $W^s(ER)$ or ER.

Case *(iii)* ($K\frac{a-c}{2b} > L$ at $K = \frac{4}{3}$). At the bifurcation value $K = \frac{4}{3}$ the segment on the diagonal bounded by $(x^E + \frac{\epsilon}{2}, x^E + \frac{\epsilon}{2})$ and (L,L) is filled with periodic points of period 2, and it is mapped to the segment bounded by $(2x^E - L, 2x^E - L)$ and $(x^E - \frac{\epsilon}{2}, x^E - \frac{\epsilon}{2})$. In particular, the 2−cycle on the border having periodic points (L,L) and $T(L,L) = (2x^E - L, 2x^E - L)$ is the only one which will survive *after the*

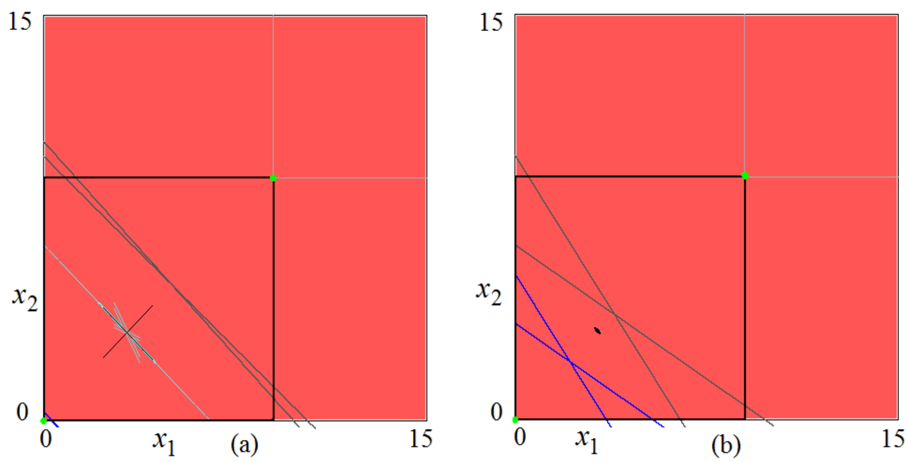

FIGURE 7. Parameters as in Fig.6 and $K = 1.9$ in (a), $K = 4.1$ in (b).

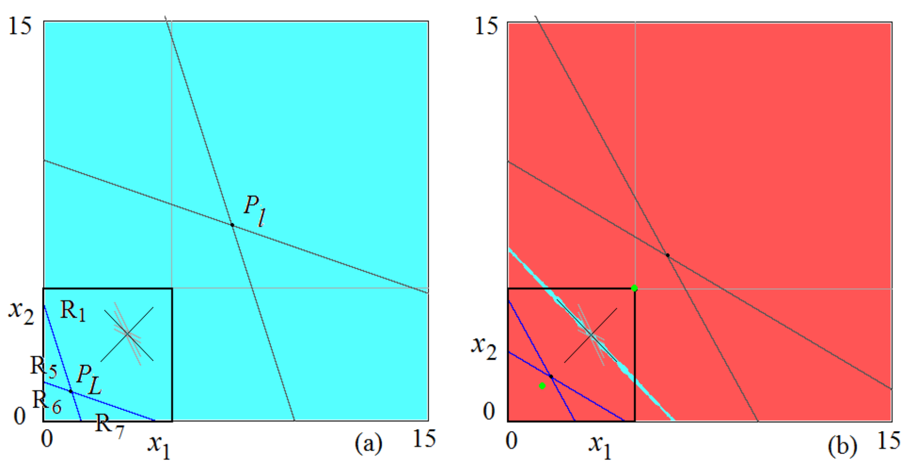

FIGURE 8. Regions of the phase plane in case (iii), at the parameter values $L = 5$, $l = .01$, $\epsilon = 0.1$, $c = 0.2$, $a = 10$, $b = 1$, and $K = 1.2$ in (a), $K = 1.4$ in (b). Inside region R_1 segments of the 4 lines determining ER are also shown, together with the eigenvectors of E. In (a) ER is globally attracting. In (b) the stable set $W^s(ER)$ is in azure while in red is the basin of attraction of the 2-cycle $(L, L) - (\frac{2-3K}{2}L + K(\frac{a-c}{2b}), \frac{2-3K}{2}L + K(\frac{a-c}{2b}))$.

bifurcation. For $K > \frac{4}{3}$ the unique attractor of the map is the 2−cycle with periodic points (L, L) and $T(L, L) = (\frac{2-3K}{2}L + K\frac{a-c}{2b}, \frac{2-3K}{2}L + K\frac{a-c}{2b})$ which belongs to the regions $R_1 - R_6$. See an example in Fig.8b, where the stable set $W^s(ER)$ is shown in azure and the basin of the 2-cycle in red. This holds with increasing K as long as a border collision bifurcation occurs, when $(L, L) = P_l$ occurring for $K = \frac{2b(L-l)}{3bL-a+c}$ after which the attracting 2−cycle is given by the corner points $(0, 0) - (L, L)$. At

$K = 4$ the transverse eigenvalue bifurcates, so that for $K > 4$ the invariant set ER becomes repelling, and all the other points converge to the 2−cycle $(0, 0) - (L, L)$.

It is simple to comment on the transition between cases (*ii*) and (*iii*), when $K\frac{a-c}{2b} = L$ at $K = \frac{4}{3}$. As we have already seen, at $K = \frac{4}{3}$ all the points not fixed on the diagonal of $\mathcal{D}$ belong to 2−cycles, and then, for any $K > \frac{4}{3}$ the attracting 2−cycle is given by the two corner points $(0, 0) - (L, L)$.

Summarizing, we have proved the following

Proposition 2 (*Dynamics in the symmetric case*)**.** *Let* $L \equiv L_1 = L_2$, $l \equiv l_1 = l_2, c \equiv c_1 = c_2, \epsilon \equiv \epsilon_1 = \epsilon_2$ *and* $K \equiv K_1 = K_2$. *Then*

(*i*) *For* $0 < K < \frac{4}{3}$, *the region* ER *is globally attracting.*

(*ii*) $\frac{2(a-c)}{3b} < L$, *and*

(*a*) $K = \frac{4}{3}$, *the segment bounded by the points* $(x^E + \frac{\epsilon}{2}, x^E + \frac{\epsilon}{2})$ *and* $P = (p_l, p_l) = (2\frac{a-c}{3b} - l, 2\frac{a-c}{3b} - l)$ *is filled with periodic points of period* 2;

(*b*) $\frac{4}{3} < K < \frac{2bL}{a-c}$, *the 2-cycle* $(0, 0) - (K\frac{a-c}{2b}, K\frac{a-c}{2b})$ *belongs to the regions* $R_1 - R_4$, *and attracts all the points not belonging to* $W^s(ER)$;

(*c*) $\frac{2bL}{a-c} \leq K < 4$, *the 2-cycle* $(0, 0) - (L, L)$ *belongs to the regions* $R_6 - R_4$, *and attracts all the points not belonging to* $W^s(ER)$.

(*iii*) $\frac{2(a-c)}{3b} > L$, *and*

(*a*) $K = \frac{4}{3}$, *the segment bounded by the points* $(x^E + \frac{\epsilon}{2}, x^E + \frac{\epsilon}{2})$ *and* (L, L) *is filled with periodic points of period* 2;

(*b*) $\frac{4}{3} < K < \frac{2b(L-l)}{3bL-a+c}$, *the 2-cycle with periodic points* (L, L) *and* $(\frac{2-3K}{2}L + K\frac{a-c}{2b}, \frac{2-3K}{2}L + K\frac{a-c}{2b})$ *belongs to the regions* $R_1 - R_6$ *and attracts all the points not belonging to* $W^s(ER)$;

(*c*) $\frac{2b(L-l)}{3bL-a+c} \leq K < 4$, *the 2-cycle* $(0, 0) - (L, L)$, *belongs to the regions* $R_6 - R_4$ *and attracts all the points not belonging to* $W^s(ER)$.

(*iv*) *For* $K > 4$ *the 2-cycle* $(0, 0) - (L, L)$ *attracts all the points not belonging to* ER.

5.2. **Model II in the general case.** In the general case, the dynamics in the phase space are not symmetric with respect to the diagonal. However, as long as the point E of model I is attracting, the region ER appears to be globally attracting in the general case as well.

At the bifurcation value when $\lambda_- = -1$, *we have segments of 2-cycles on the eigenvector* e_-, belonging to region R_1, and the closest border determines which region will have the attracting 2−cycle when $\lambda_- < -1$.

Let us describe, via a few examples, how the attracting 2-cycle and the related bifurcations can be determined.

As a first example, we consider the same parameters used in Fig.4a, with $K_1 = 0.9$, and varying K_2. The bifurcation $\lambda_- = -1$ occurs at $K_2 = \frac{8.8}{5.3} = 1.660377...$ and the closest region is R_2. Therefore, when $\lambda_- < -1$, there will be a 2-cycle belonging to the regions $R_1 - R_2$. As a point in R_2 is mapped into a point $(x_1^*, 0)$ we can determine the attracting 2-cycle analytically. As $T(x_1^*, 0) = (f_1(x_1^*, 0), f_2(x_1^*, 0))$ the 2−cycle must satisfy $T^2(x_1^*, 0) = (x_1^*, 0)$ and thus

$$x_1^* = f_1(f_1(x_1^*, 0), f_2(x_1^*, 0)) \tag{48}$$

leading to

$$x_1^* = \frac{4}{8 - 4K_1 - K_2}\left((2 - K_1)\frac{a - c_1}{2b} - \frac{K_2}{2}\frac{a - c_2}{2b}\right). \tag{49}$$

For $K_2 = 1.67$ an example is shown in Fig.9a. As K_2 increases, the periodic point $(x_1^*, 0)$ approaches the border (r_c) and its image $T(x_1^*, 0) = (f_1(x_1^*, 0), f_2(x_1^*, 0))$ approaches the upper boundary $x_2 = L_2$. The bifurcation occurs when $(x_1^*, 0) \in (r_c)$ leading to

$$\hat{K}_2 = \frac{4L_2(2 - K_1)}{L_2 + (2 - K_1)(2\frac{a-c_2}{b} - \frac{a-c_1}{b})}. \tag{50}$$

If $K_1 = 0.9$, we have $\hat{K}_2 \cong 2.002$. For $K_2 > \hat{K}_2$ the 2-cycle has the periodic point $(x_1^*, 0)$ belonging to region R_5 thus the attracting 2-cycle is in the regions $R_5 - R_2$ with periodic points $(x^*, 0) - ((f_1(x^*, 0), L_2)$ where x^* satisfies

$$x^* = f_1(f_1(x^*, 0), L_2) \tag{51}$$

leading to

$$x^* = \frac{a - c_1}{2b} - \frac{L_2}{2(2 - K_1)} \tag{52}$$

An example is shown in Fig.9b. This 2-cycle $(x^*, 0) - ((f_1(x^*, 0), L_2)$ persists for any $K_2 > \hat{K}_2$ (as it no longer depends on K_2).

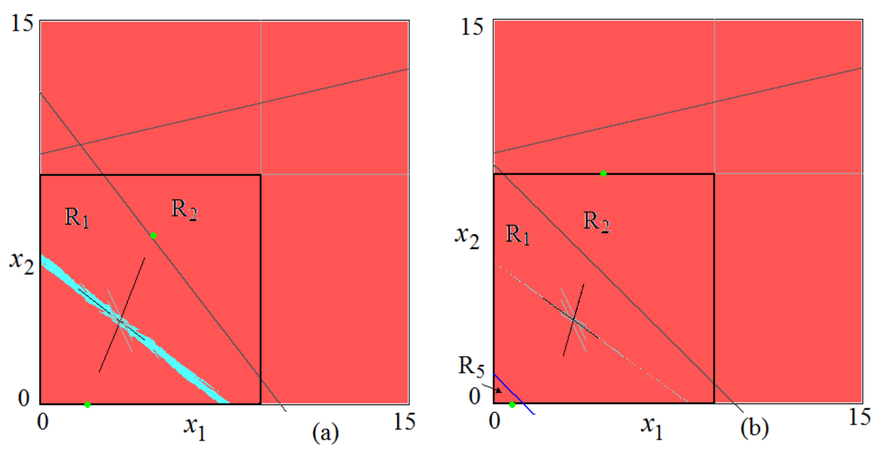

FIGURE 9. Phase plane at the parameter values $L_1 = L_2 = 9$, $l_1 = l_2 = .01$, $\epsilon_1 = \epsilon_2 = 0.1$, $c_1 = c_2 = 0.2$, $a = 10$, $b = 1$, $K_1 = 0.9$, and $K_2 = 1.67$ in (a), $K_2 = 2.1$ in (b).

For a different value of K_1, the attracting 2-cycle undergoes two border collision bifurcations as K_2 increases. As a second example we consider the same parameters used in Fig.4b, with $K_1 = 1.2$ and varying K_2. The bifurcation $\lambda_- = -1$ occurs at $K_2 = \frac{1.6}{1.1} = 1.\overline{45}$ and leads to a 2-cycle belonging to the regions $R_1 - R_2$ given by $(x_1^*, 0) \in R_1$ and $T(x_1^*, 0) = (f_1(x_1^*, 0), f_2(x_1^*, 0)) \in R_2$ where x_1^* has been defined in (49) (see Fig.10a). Now at this bifurcation, four regions belong to the rectangle $\mathcal{D}$, as shown in Fig.10a.

The attracting 2-cycle undergoes another border collision when $T(x_1^*, 0)$ belongs to the straight line (r_b) which also corresponds to the collision $(x_1^*, 0) = (0, 0)$ and occurs for

$$\widetilde{K}_2 = 2(2 - K_1)\frac{a - c_1}{a - c_2} \tag{53}$$

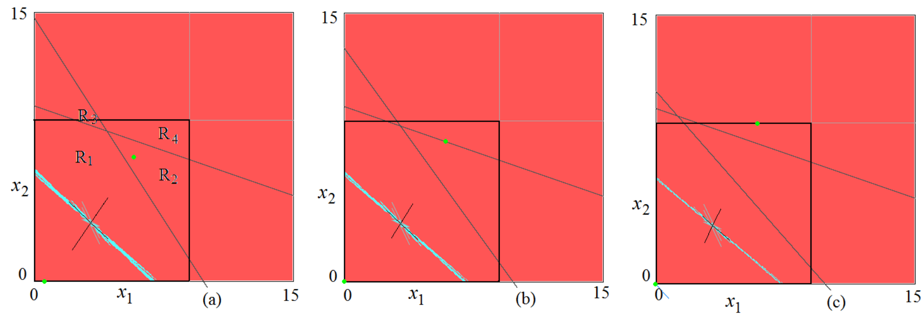

FIGURE 10. Phase plane at the parameter values $L_1 = L_2 = 9$, $l_1 = l_2 = .01$, $\epsilon_1 = \epsilon_2 = 0.1$, $c_1 = c_2 = 0.2$, $a = 10$, $b = 1$, $K_1 = 1.2$, and $K_2 = 1.5$ in (a), $K_2 = 1.6$ in (b), $K_2 = 1.836735$ in (c).

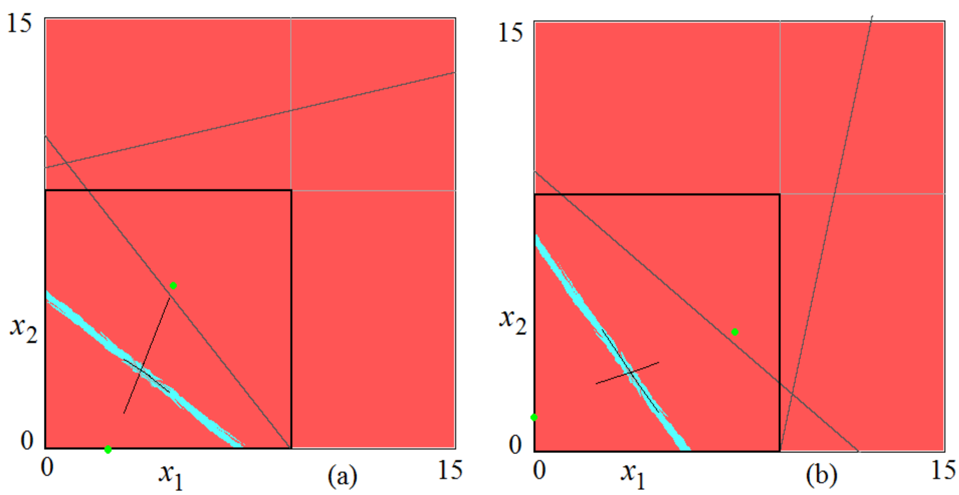

FIGURE 11. Phase plane at the parameter values $L_1 = L_2 = 9$, $l_1 = l_2 = .01$, $\epsilon_1 = \epsilon_2 = 0.1$, $c_1 = 0.2$, $c_2 = 1$, $a = 10$, $b = 1$, and $K_1 = 0.9$, $K_2 = 1.7$ in (a), $K_1 = 1.7$, $K_2 = 0.9$ in (b).

For $K_1 = 1.2$, we find that $\widetilde{K}_2 = 1.6$ (see Fig.10b). At this collision, and after, the attracting 2-cycle belonging to the regions $R_1 - R_4$ is given by

$$(0,0) - (K_1 \frac{a-c_1}{2b}, K_2 \frac{a-c_2}{2b}). \tag{54}$$

By increasing K_2, the periodic point $(K_1 \frac{a-c_1}{2b}, K_2 \frac{a-c_2}{2b})$ approaches the upper line $x_2 = L_2$ and the contact occurs when $(0,0) \in (r_c)$ leading to $K_2(\frac{a-c_2}{2b}) = L_2$ that is

$$\overline{K}_2 = \frac{2bL_2}{a-c_2}. \tag{55}$$

In our example, we get $\overline{K}_2 = 1.83673...$ (see Fig.10c). For any $K_2 > \overline{K}_2$ the attracting 2-cycle belongs to the regions $R_5 - R_4$ and is given by

$$(0,0) - (K_1 \frac{a - c_1}{2b}, L_2) \tag{56}$$

We notice that the two examples considered above for different values of $(K_1, K_2) = (\xi, \eta)$ are in the case described in **Property 1** (as $L_1 = L_2$, $l_1 = l_2$, $c_1 = c_2$ and $\epsilon_1 = \epsilon_2$), so using examples with $(K_1, K_2) = (\eta, \xi)$ we get cycles which are symmetric with respect to the diagonal $(x_1 = x_2)$ of the phase plane. For example, for $(K_1, K_2) = (0.9, 1.67)$ the attracting $2-$cycle is $(1.90256, 0) - (4.60026, 6.59436)$, so that for $(K_1, K_2) = (1.67, 0.9)$ the attracting 2-cycle is $(0, 1.90256) - (6.59436, 4.60026)$.

However, in the asymmetric case this is clearly no longer true (For example, see Fig.11), but the local stability is not affected (as it depends only on K_1 and K_2 and the eigenvalues are unchanged unlike the eigenvectors). The reasoning on the bifurcations occurring to the periodic points of the attracting $2-$cycle as a function of the parameters is similar to the one performed in the previous examples.

As remarked above, when the invariant set ER is not attracting the $2-$cycle must have the two periodic points in two different regions, at least one periodic point must belong to the border of the region $\mathcal{D}$ (with one constant $x_i = L_i$ or $x_i = 0$) and whenever one of the periodic points crosses a border defined by the lines (r_k) the $2-$cycle changes its definition. The number of lines which can be crossed depends on the regions R_j with a portion in the absorbing rectangle $\mathcal{D}$. Ultimately the $2-$cycle must have both two periodic points on the border of the region $\mathcal{D}$.

6. **Conclusion.** In this paper we have introduced a realistic assumption into a well-known oligopoly model, as defined in the baseline model. If the demand and all cost functions are linear, then the additional assumptions result in the loss of the linearity and the continuity of the dynamic model and the uniqueness of the steady state. Although in model II there are infinitely many steady states, defining a whole region ER, the invariant set ER is attracting under the same conditions of the baseline model. Clearly model II restricts and bounds the possible output values; therefore leads to a different behavior when the invariant region ER is not attracting. In the symmetric case all existing attracting $2-$cycles are fully determined in Section 4.2. In the general case there are many possibilities, depending on the parameters. However, we have shown how to detect analytically the periodic points of the attracting $2-$cycle, having at least one periodic point (or both) on the borders of the absorbing rectangle $\mathcal{D}$.

The results show that with the added nonlinear constraints, we lost the ability to predict future outputs precisely at the unique steady state; however, for a moderately small speeds of adjustment K_1 and K_2 we can still expect the outputs in the long run to be in a steady state set, ER. When the speeds of adjustment are outside the stability region, the dynamics of model II become two-cyclical. For the symmetric duopoly case, we find that firms will either be both producing nothing or both producing at the amount that is equal to the monopoly output (in the static model) multiplied by the speed of adjustment or at the capacity limit. This result may first seem surprising but actually quite intuitive since firms are best responding to the rival firm's output level in the previous period. A firm will choose to produce at the monopoly level, while bounded by the capacity limit and adjusted by K, in the current period when the rival firm produced nothing in the last period. A similar result holds for the asymmetric case.

Without adaptive learning in the speed of adjustment parameters (as assumed in this paper), it may be best for the government to ensure that a small enough K is used by the firms to avoid the outcome swinging between nothing is produced or a total amount greater than the competitive equilibrium is produced.

For the future study, we plan to examine the dynamics of the system with a flexible capacity limit constraints, as a percentage of the current output levels. Interestingly, the dynamics and bifurcations become much richer, leading also to chaotic behaviors.

REFERENCES

[1] R. Amir, Cournot oligopoly and the theory of supermodular games, *Games and Economic Behavior,* **15** (1996), 132–148.

[2] R. Amir and V. E. Lambson, On the effects of entry in Cournot markets, *Review of Economic Studies,* **67** (2000), 235–254.

[3] G. I. Bischi, C. Chiarella, M. Kopel and F. Szidarovszky, Nonlinear Oligopolies: Stability and Bifurcations, Springer-Verlag, Berlin-Heidelberg-New York, 2010.

[4] G. I. Bischi, L. Gardini and U. Merlone, Impulsivity in binary choices and the emergence of periodicity, *Discrete Dynamics in Nature and Society,* (2009), Article ID 407913, 22 pages.

[5] A. Dal Forno, L. Gardini and U. Merlone, Ternary choices in repeated games and border collision bifurcations, *Chaos Solitons & Fractals,* **45** (2012), 294–305.

[6] R. Day, *Complex Economic Dynamics*, MIT Press, Cambridge, 1994.

[7] M. di Bernardo, C. J. Budd, A. R. Champneys and P. Kowalczyk, *Piecewise-smooth Dynamical Systems: Theory and Applications*, Applied Mathematical Sciences 163, Springer-Verlag, London, 2008.

[8] T. Bresnahan and V. Ramey, Output Fluctuations at the Plant Level, *Quaterly Journal of Economics,* **109** (1994), 593–624.

[9] C. Fershtman and M. Kamien, Dynamic duopolistic competition with sticky prices, *Econometrica,* **55** (1987), 1151–1164.

[10] L. Gardini, I. Sushko and A. Naimzada, Growing through chaotic intervals, *Journal of Economic Theory,* **143** (2008), 541–557.

[11] L. Gardini, U. Merlone and F. Tramontana, Inertia in binary choices: Continuity breaking and big-bang bifurcation points, *Journal of Economic Behavior & Organization,* **80** (2011), 153–167.

[12] W. Huang and R. Day, Chaotically switching bear and bull markets: The derivation of stock price distributions from behavioral rules, in *Nonlinear Dynamics and Evolutionary Economics* (eds. R. Day, and P. Chen), Oxford University Press, 1993.

[13] W. Novshek, On the existence of Cournot equilibrium, *Review of Economic Studies,* **52** (1985), 85–98.

[14] H. E. Nusse and J. A. Yorke, Border-collision bifurcations including period two to period three for piecewise smooth systems, *Physica D,* **57** (1992), 39–57.

[15] H. E. Nusse and J. A. Yorke, Border-collision bifurcation for piecewise smooth one-dimensional maps, *Int. J. Bifurcation Chaos,* **5** (1995), 189–207.

[16] K. Okuguchi, *Expectations and Stability in Oligopoly Models*, Springer-Verlag, Berlin-Heidelberg-New York, 1976.

[17] K. Okuguchi and F. Szidarovszky, *The Theory of Oligopoly with Multi-product Firms*, Lecture Notes in Economics and Mathematical Systems, 342, Springer-Verlag, Berlin, 1990.

[18] T. Puu and I. Sushko (eds.), *Oligopoly Dynamics, Models and Tools*, Springer Verlag, New York, 2002.

[19] T. Puu and I. Sushko (eds.), *Business Cycle Dynamics, Models and Tools*, Springer Verlag, New York, 2006.

[20] D. Radi, L. Gardini and V. Avrutin, The role of constraints in a segregation model: The symmetric case, *Chaos, Solitons & Fractals,* **66** (2014), 103–119.

[21] D. Radi, L. Gardini and V. Avrutin, The role of constraints in a segregation model: The asymmetric Case *Discrete Dynamics in Nature and Society,* (2014), Art. ID 569296, 17 pp.

[22] M. Simaan and T. Takayama, Game theory applied to dynamic duopoly problems with production constraint, *Automatica,* **14** (1978), 161–166.

[23] I. Sushko and L. Gardini, Degenerate bifurcations and border collisions in piecewise smooth 1D and 2D maps, *Int. J. Bif. and Chaos,* **20** (2010), 2045–2070.

[24] I. Sushko, L. Gardini and K. Matsuyama, Superstable credit cycles and u-sequence, *Chaos Solitons & Fractals,* **59** (2014), 13–27.

[25] F. Tramontana, F. Westerhoff and L. Gardini, On the complicated price dynamics of a simple one-dimensional discontinuous financial market model with heterogeneous interacting traders, *J. Econ. Behav. Organ.,* **74** (2010), 187–205.

[26] F. Tramontana, L. Gardini and F. Westerhoff, Heterogeneous speculators and asset price dynamics: Further results from a one-dimensional discontinuous piecewise-linear model, *Computational Economics,* **38** (2011), 329–347.

[27] Z. T. Zhusubaliyev and E. Mosekilde, *Bifurcations and Chaos in Piecewise-Smooth Dynamical Systems*, World Scientific, Singapore, 2003.

Received October 2014; revised March 2015.

E-mail address: chrystie.burr@colorado.edu
E-mail address: laura.gardini@uniurb.it
E-mail address: szidarka@gmail.com